THE 3543 CM^{-1} INFRARED ABSORPTION BAND IN NATURAL AND SYNTHETIC AMETHYST AND ITS VALUE IN IDENTIFICATION

Vladimir S. Balitsky, Denis V. Balitsky, Galina V. Bondarenko, and Olga V. Balitskaya

The proper use and limitations of IR spectroscopy for identifying natural versus synthetic amethyst of various types have been investigated, focusing on the region 3800–3000 cm^{-1}. The presence of absorption bands at approximately 3680, 3664, and 3630 cm^{-1} unambiguously proves artificial origin, but only for samples grown in near-neutral NH_4F solutions. Conversely, there are no unambiguous diagnostic features in the IR spectra of the more commercially significant synthetic amethyst grown in alkaline K_2CO_3 solutions. Nevertheless, previous investigators have found potential diagnostic value in absorption bands at approximately 3595 and 3543 cm^{-1}. Although the 3595 cm^{-1} band is not found in the spectra of synthetic amethyst, it also is frequently absent from those of natural amethyst. The 3543 cm^{-1} band is found in the vast majority of synthetic amethysts grown in alkaline solutions, but this band also is sometimes present in natural amethyst—so it provides only tentative evidence of synthetic origin. Moreover, the 3543 cm^{-1} band is absent from some varieties of synthetic amethyst. The unambiguous identification of natural versus synthetic amethyst therefore must be based on a combined examination of the IR spectra, internal growth structures (including twinning), and inclusions.

Recently, we have studied in detail the relationship between conditions of formation and the absorption spectra of natural and synthetic amethyst in the 3800–3000 cm^{-1} region to determine whether infrared spectroscopy can be used to identify synthetic origin (see Balitsky et al., 2003, 2004). Previously it was shown that both natural amethyst and synthetic amethyst grown in alkaline solutions share similar spectral features in this region (Balakirev et al., 1979; Zecchini, 1979; Balitsky, 1980; Lind and Schmetzer, 1980; Zecchini and Smaali, 1999). Two absorption bands are almost always present in both types—an intense feature at 3585 cm^{-1} and a relatively weak one at 3612 cm^{-1}—due to the presence of OH^- defects in the quartz structure (Rossman, 1988). Also characteristic is a broad band with a maximum near 3400 cm^{-1}, which often overlaps the absorption bands mentioned above, that is related to the presence of molecular water (Kats, 1962; Rossman, 1988). In addition, the IR spectra of some natural amethyst exhibits an absorption band at 3595 cm^{-1} that is never found in the spectra of synthetic amethyst (Zecchini, 1999). There are also indications that an absorption band near 3543 cm^{-1} occurs rarely in the IR spectra of natural amethyst, but is present in the overwhelming majority of synthetic amethysts (Fritsch and Koivula, 1987; Fritsch and Rossman, 1990; Zecchini and Smaali, 1999).

Thus, the 3543 cm^{-1} band has become established as one of the basic features indicative of synthetic origin in amethyst. However, it has been shown recently that this band commonly occurs in

See end of article for About the Authors and Acknowledgments.
GEMS & GEMOLOGY, Vol. 40, No. 2, pp. 146–161.

Figure 1. Large quantities of synthetic amethyst are present in the gem trade, but challenges remain in separating this material from its natural counterpart. In some cases, infrared spectroscopy may provide evidence of natural or synthetic origin. The synthetic amethyst in this suite of jewelry is set with diamonds (and opal in the ring); the oval checkerboard cut in the pendant weighs 4.91 ct, and the loose samples are 1.94, 1.18, and 0.73 ct (GIA Collection nos. 20662, 20664, and 20665, respectively). Jewelry courtesy of Gems of La Costa, Carlsbad, California; photo by Maha Tannous.

the IR spectra of natural amethyst from the Caxarai mine in Brazil (Kitawaki, 2002). According to our own data, this band also is present in some amethyst from other localities.

These factors have created uncertainty with respect to the usefulness of IR spectroscopy in general, and the 3543 cm^{-1} band in particular, for identifying the natural or synthetic origin of amethyst. Given the quantity of synthetic amethyst in the jewelry market (figure 1), we performed the present study to investigate the characteristics of the 3543 cm^{-1} band in various growth sectors of synthetic amethyst manufactured under different conditions, as well as the effects of growth rate, crystallographic orientation, gamma irradiation, and annealing on this band.

THE MORPHOLOGY AND INTERNAL GROWTH STRUCTURE OF SYNTHETIC AMETHYST

To provide a better understanding of the results of this investigation, we will first consider some features of the morphology and internal structure of synthetic amethyst crystals grown on seed plates of various orientations, and compare them to those of natural quartz (figure 2). Crystals of natural quartz commonly show faces of the hexagonal prism *m* $\{10\bar{1}0\}$, positive rhombohedron *r* $\{10\bar{1}1\}$, and negative rhombohedron *z* $\{01\bar{1}1\}$ (figure 2A). In addition, faces of the trigonal trapezohedron *x* $\{51\bar{6}1\}$ and trigonal dipyramid +*s* $\{11\bar{2}1\}$ may be present. In general, the particular faces present on synthetic amethyst crystals depend on the orientation and size of the seed plate, as well as on the growth rate and duration. As a rule, the *m*, *r*, and sometimes *z* faces are common for synthetic amethyst grown in alkaline solutions on the seeds cut parallel to *z*, *r*, and the basal pinacoid *c* {0001} (figure 2B). However, the *m*, *r*, *z*, +*s*, positive trigonal prism +*a* $\{11\bar{2}0\}$, and negative trigonal prism –*a* $\{2\bar{1}\bar{1}0\}$ faces are typical for synthetic amethyst grown in NH_4F solutions on seeds cut parallel to *c* and *s* faces (figure 2C). The trigonal prism faces are found between those of the hexagonal prism, perpendicular to the X-axis. These faces are rarely present on natural quartz crystals (Dana et al., 1962), but they are commonly found on synthetic quartz (including crystals grown in NH_4F solutions on seeds cut parallel to *c* and *s* with ZY orientation).

The growth of synthetic amethyst in alkaline solutions takes place mainly on seed plates cut parallel to *z* and, very rarely, on seeds cut parallel to *r* (Balakirev et al., 1979; Balitsky, 1980; Balitsky and Lisitsina, 1981). Such crystals usually have an elongate tabular form (figure 3A). When the *z*-seed is used, the crystals are dominated by *z* and *m* faces, and also show smaller *r* faces. The *z* growth sectors are of primary importance in such crystals; only rarely do they contain significant *r* sectors, and *m*

growth sectors are absent (figure 3B). These crystals sometimes contain spindle-shaped Dauphiné *r*-twins within the *z* sectors (see, e.g., the plate at the bottom of figure 3B). The same morphology and growth structure have been seen in Japanese and Chinese synthetic amethyst grown under equivalent conditions (figure 4).

When the *r*-seed is used, the crystals show *r* and *m* faces (figure 5), and the *z* faces (and sectors) are typically absent. The *r* sectors almost always contain polysynthetic Brazil twins (see figure 5, inset).

Very rarely, synthetic amethyst crystals are grown on seeds cut parallel to *c* or on seeds with an unconventional orientation. These crystals are characterized by morphological and color-distribution characteristics that differ from those described above. For example, crystals grown on seeds cut parallel to *c* may have a tabular shape with well-developed *m*, *r*, and *z* faces (figure 6). Such crystals typically consist of bicolored synthetic amethyst-citrine, with the amethyst portion formed by both *z* and *r* sectors. When the seed plates used are nearly cubic in shape, the grown crystals acquire a prismatic habit with an even distribution of *r*, or *r* and *z* sectors (figure 7). These crystals may yield faceted synthetic amethyst of high quality (figure 8).

The growth of synthetic amethyst in near-neutral NH_4F solutions is done on seed plates cut parallel to *c* or *s* (Balitsky, 1980; Balitsky et al., 2000). The crystals are elongated on the Y- or X-axis, and their particular habit and internal structure are defined by the orientation of the seed plates and the growth rates of the main faces (i.e., *c*, *+s*, and *+a*; figures 9 and 10). In contrast to crystals grown in alkaline solutions, the *z* and *r* sectors are insignificant, and there are practically no *m* faces.

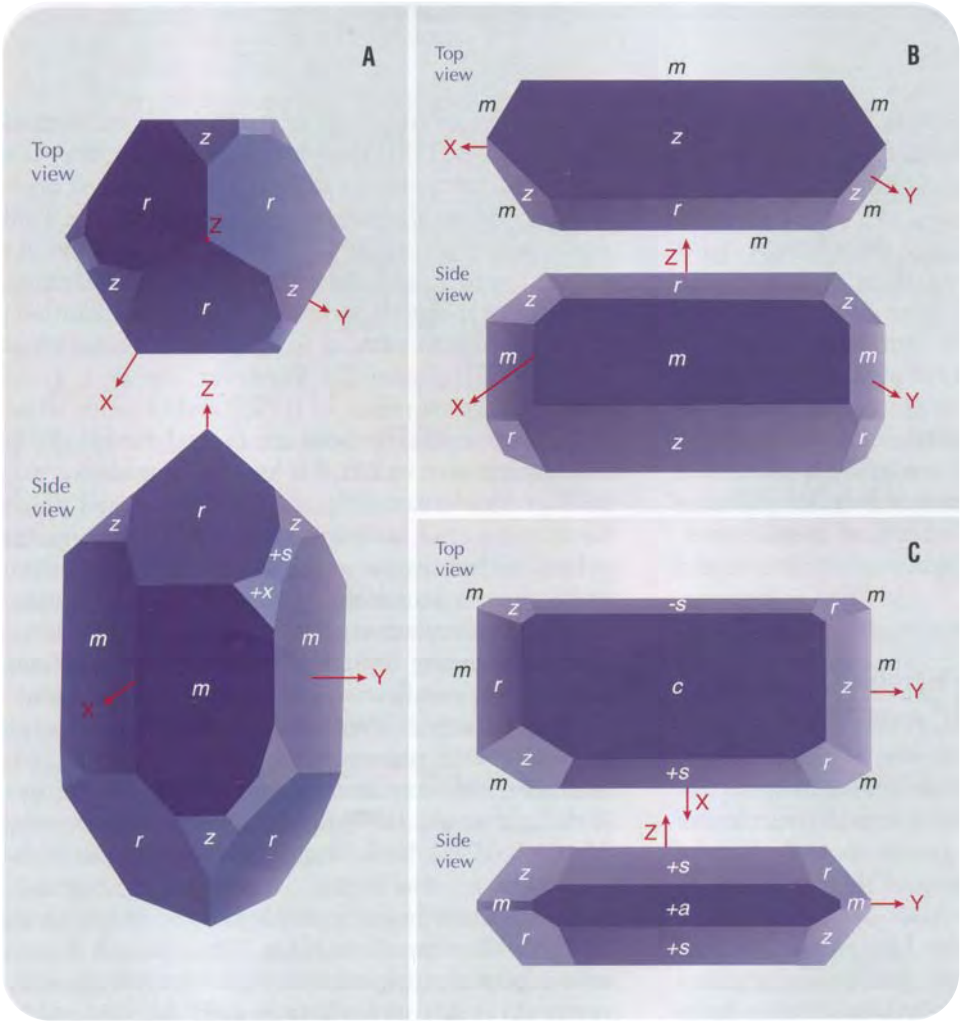

Figure 2. These drawings show the principal faces and crystallographic axes for natural quartz (A) and synthetic amethyst grown in alkaline K_2CO_3 solution on a seed cut parallel to z *(B) and in near-neutral NH_4F solution on a seed cut parallel to* c *or* s *(C). The notation of X, Y, and Z axes follows the convention used by crystal growth technologists for an orthogonal coordinate system (in contrast, most mineralogists refer to a_1, a_2, a_3, and c axes for the hexagonal crystal system). The labels* r *and* z *refer to faces of positive and negative rhombohedra, respectively, and the hexagonal prism is* m. *Some faces have positive or negative designations, depending on their location relative to the X and Y axes; this is the case for the trigonal trapezohedron* x, *the trigonal bipyramid* s, *and the trigonal prism* a. *Natural quartz crystals rarely show the trigonal prism* a, *and typically do not have* c *faces, which are oriented perpendicular to the Z (optic) axis.*

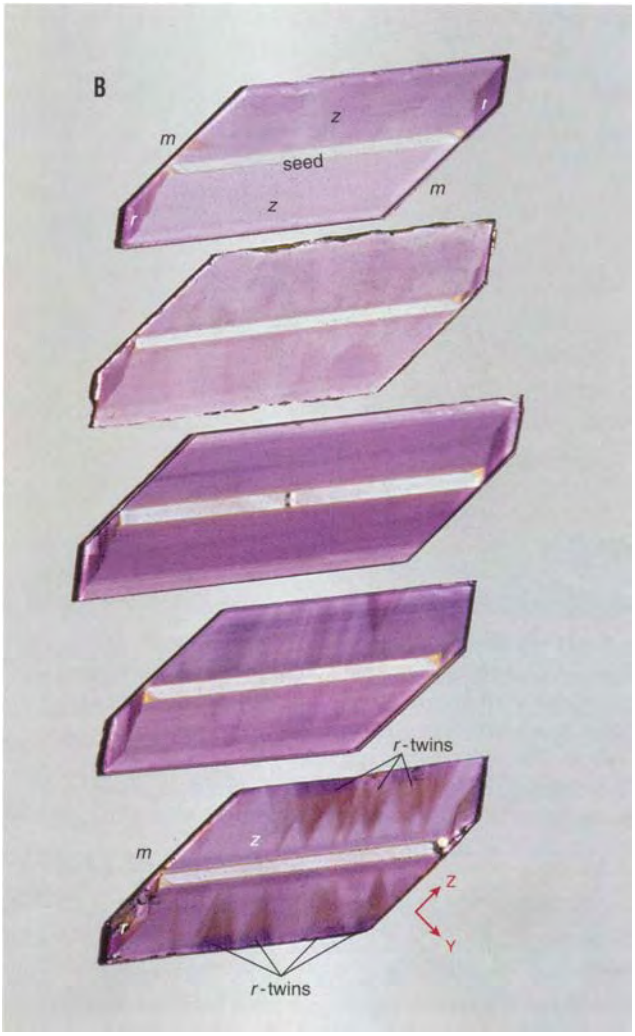

Figure 3. The synthetic amethyst crystals in image A show the typical morphology resulting from growth in alkaline K_2CO_3 solutions on seeds cut parallel to z*; the largest crystal is 23 cm long. Image B shows polished slices that were cut from such crystals (2 mm thick, sliced parallel to* a*). Note the colorless seed plate along the center of each slice. The crystals are formed mainly by* z *growth sectors, while* r *sectors occupy small portions. Faceted synthetic amethysts prepared from such crystals consist almost entirely of the* z *sector. However, Dauphiné twinning may augment the* r *sectors in such crystals (see bottom slice), so that faceted material may contain both* z *and* r *sectors. Photos by V. S. Balitsky (image A) and Maha Tannous (image B).*

MATERIALS AND METHODS

To ensure reliable results, we studied a total of 238 commercially available samples of hydrothermal synthetic amethyst that were grown by us under known and controlled conditions, at facilities in Aleksandrov (VNIISIMS) and Chernogolovka (IEM RAS). This included a core group of 120 crystals (0.3–12 kg each) and slices cut from them, most of which were grown in alkaline K_2CO_3 solutions at temperatures of 300–350°C and pressures of 1000–1500 atm in the presence of Fe^{3+} and an oxidizer (Balitsky and Lisitsina, 1981). The seed plates in these samples mainly were cut parallel to *z*, as is the case for most of the synthetic amethyst in the gem trade. However, eight additional crystals (0.2–0.4 kg each) were grown in these solutions on seeds cut parallel to *r*, and more than 50 crystals were grown on seeds cut parallel to *c* in conjunction with a

Figure 4. These crystals of synthetic amethyst were grown in the 1980s in China (left, 8.5 cm long) and Japan (right, 12 cm long). They show identical morphologic features to those of the Russian samples in figure 3, and were apparently produced under equivalent conditions. Photos by V. S. Balitsky.

Figure 5. Synthetic amethyst crystals grown in alkaline K_2CO_3 solutions on seed plates cut parallel to r *are dominated by* r *sectors. The 2-mm-thick plate on the bottom was sliced parallel to* a *from a similar crystal. The inset shows numerous polysynthetic Brazil twins in the* r *sector, which were brought out by etching the slab in a strong $NH_4F \cdot HF$ solution. Photos by V. S. Balitsky.*

Figure 6. These synthetic quartz crystals were grown in alkaline solutions on seeds cut parallel to c*, and show well-developed* m*,* r*, and* z *faces. The two crystals on top are shown before gamma irradiation and those on the bottom, after irradiation to create the amethyst coloration (the largest crystal measures 21 × 7 cm). The inset shows a slice through the upper portion of a synthetic ametrine crystal (2 mm thick, cut parallel to* a*), which consists of the* z *and* r *sectors. Synthetic amethyst faceted from such material will include both of these sectors, and therefore will show varying behavior of the 3543 cm^{-1} absorption band. Photos by Maha Tannous and D. V. Balitsky (inset).*

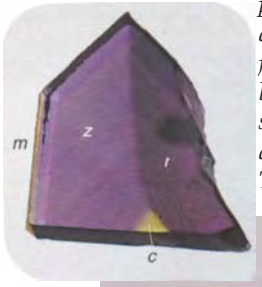

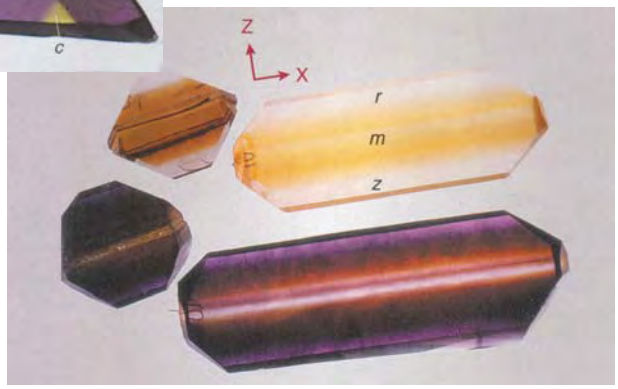

Figure 7. Prismatic crystals of synthetic amethyst are grown in alkaline solutions on seeds that are nearly cubic in shape. Such crystals have well-developed m*,* r*, and* z *faces, and their morphology closely resembles that of natural quartz crystals. The yellow color in the center of the prism correlates to* c *sectors, whereas the amethyst areas consist of rhombohedral sectors. Photos by V. S. Balitsky.*

metal mask containing holes of 10–50 mm in diameter. In the latter case, it was possible to grow prismatic crystals that were very similar to natural amethyst in terms of morphology and internal growth structure (Balitsky and Balitskaya, 1985; Balitsky et al., 1999).

Also used in this study were 30 synthetic amethyst crystals (0.2–1.2 kg each) that we grew in NH_4F solutions (Balitsky, 1980; Balitsky et al., 2000) at temperatures of 240–350°C and pressures of 80–300 atm, on seeds cut parallel to *c* and *s*. In addition, we studied more than 80 crystals of bicolored synthetic amethyst-citrine (0.3–0.7 kg each), grown in K_2CO_3 solutions under the same conditions that are used to produce commercial amethyst, but on seed plates cut parallel to *c*.

A few synthetic amethyst crystals from China (four samples) and Japan (three) also were studied.

To achieve the purple amethyst color, all of the crystals—which were colorless or pale yellow to yellow as grown—were subjected to ionizing radiation (5 megarads of gamma rays from a ^{60}Co source). Color stability was tested by heating 53 of the samples in the 310–700°C range for 1–4 hours.

IR spectra (in the 3800–3000 cm^{-1} region) were recorded on all of the samples, before and after irradiation; we used a Nicolet Avatar 320 FTIR spectrometer at room temperature, with an unpolarized beam. A total of 580 spectra of synthetic amethyst grown in alkaline solutions, and more than 50 spectra of samples grown in near-neutral solutions, were recorded. The samples were prepared as polished plates (2–10 mm thick) cut parallel to *x*, *c*, and, more rarely, to unoriented surfaces. Typically one slice was prepared from each crystal. However, several plates were cut from some crystals so that the IR spectra could be recorded in different orientations. In addition, one cube-shaped sample (10 mm on each side) of synthetic amethyst grown in an alkaline solution was prepared for spectroscopy with the edges oriented parallel to the X, Y, or Z axes.

The IR spectra of 52 samples of natural amethyst from the following localities also were recorded: Caxarai mine in Rondonia State (4 samples) and unspecified deposits (10) in Rio Grande do Sul State, Brazil; Anahí mine, Bolivia (9); Vatikha deposit, Middle Ural Mountains, Russia (14); Khasavarka deposit, Polar Urals, Russia (6); Angarskoye deposit, central drainage basin of Angara River, eastern Siberia, Russia (2); and the Rhodope Mountains, Bulgaria (7). The samples consisted of polished plates (2–4 mm thick) cut parallel to *c*, *m*, and *a*.

Figure 8. The ends of the prismatic crystals can be faceted to yield high-quality synthetic amethyst, which will consist of both z *and* r *sectors. The crystal termination measures 2.4 cm high. Photo by Maha Tannous.*

RESULTS AND DISCUSSION

Our study confirmed the findings of numerous investigators who have compared the IR spectra (including the 3543 cm^{-1} band) of natural amethyst to its synthetic counterpart grown in alkaline solutions (see, e.g.,

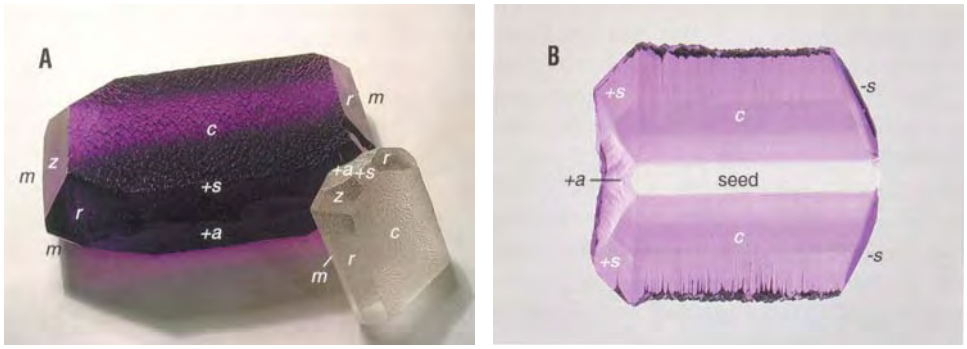

Figure 9. Image A shows synthetic quartz crystals (before and after irradiation) grown in NH_4F solutions on seeds cut parallel to c. *Image B shows the growth sectors in a 2.5-mm-thick plate that was sliced parallel to* m. *The crystals are dominated by* c *sectors, with subordinate* +a, +s, *and* –s *sectors. Photos by V. S. Balitsky.*

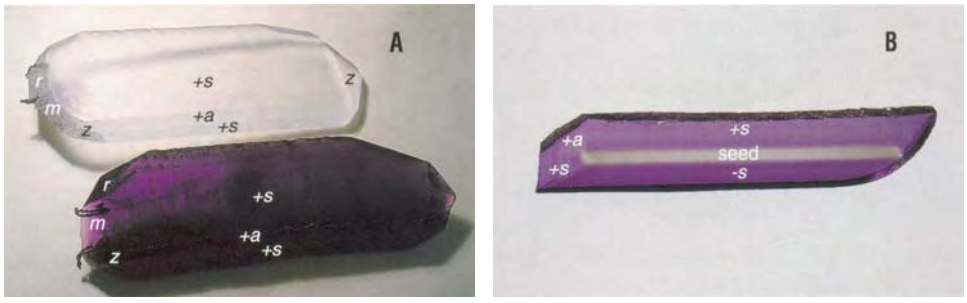

Figure 10. Image A shows synthetic quartz crystals (before and after irradiation) grown in NH_4F solutions on seeds cut parallel to s. *As depicted in image B of a 4-mm-thick plate that was sliced parallel to* m, *the dominant growth sectors are* +s *and* –s, *and* +a *is subordinate. Photos by V. S. Balitsky.*

Zecchini, 1979; Zecchini and Smaali, 1999; Balakirev et al., 1979; Balitsky and Lisitsina, 1981; Fritsch and Koivula, 1987; Fritsch and Rossman, 1990; Kitawaki, 2002). The 3543 cm^{-1} band is typically absent from the spectra of natural amethyst, except in samples from Brazil's Caxarai deposit (Kitawaki, 2002), as well as in some samples from other localities (e.g., Brazil's Rio Grande do Sul State; Bulgaria's Rhodope Mountains; and Russia's Khasavarka and Angarskoye deposits; see figure 11). Furthermore, the occurrence of this band varies according to different growth sectors and zones within a given crystal. Note, however, that we did not observe this peak in the spectra that we recorded of samples from the Vatikha deposit.

For comparison, the presence or absence of the 3543 cm^{-1} band in the IR spectra of synthetic quartz grown in alkaline solutions will be covered below. The unusual IR spectra shown by synthetic amethyst grown in near-neutral NH_4F solutions will be discussed at the end of this section.

Our observations suggest that the presence or absence of the 3543 cm^{-1} band reflects certain conditions of crystal growth common to both natural and synthetic amethyst. It appears that the most important factors are those related to the formation of amethyst and citrine color centers—that is, structural (amethyst) and nonstructural (citrine) impurities of Fe^{3+} (Balitsky and Balitskaya, 1985).

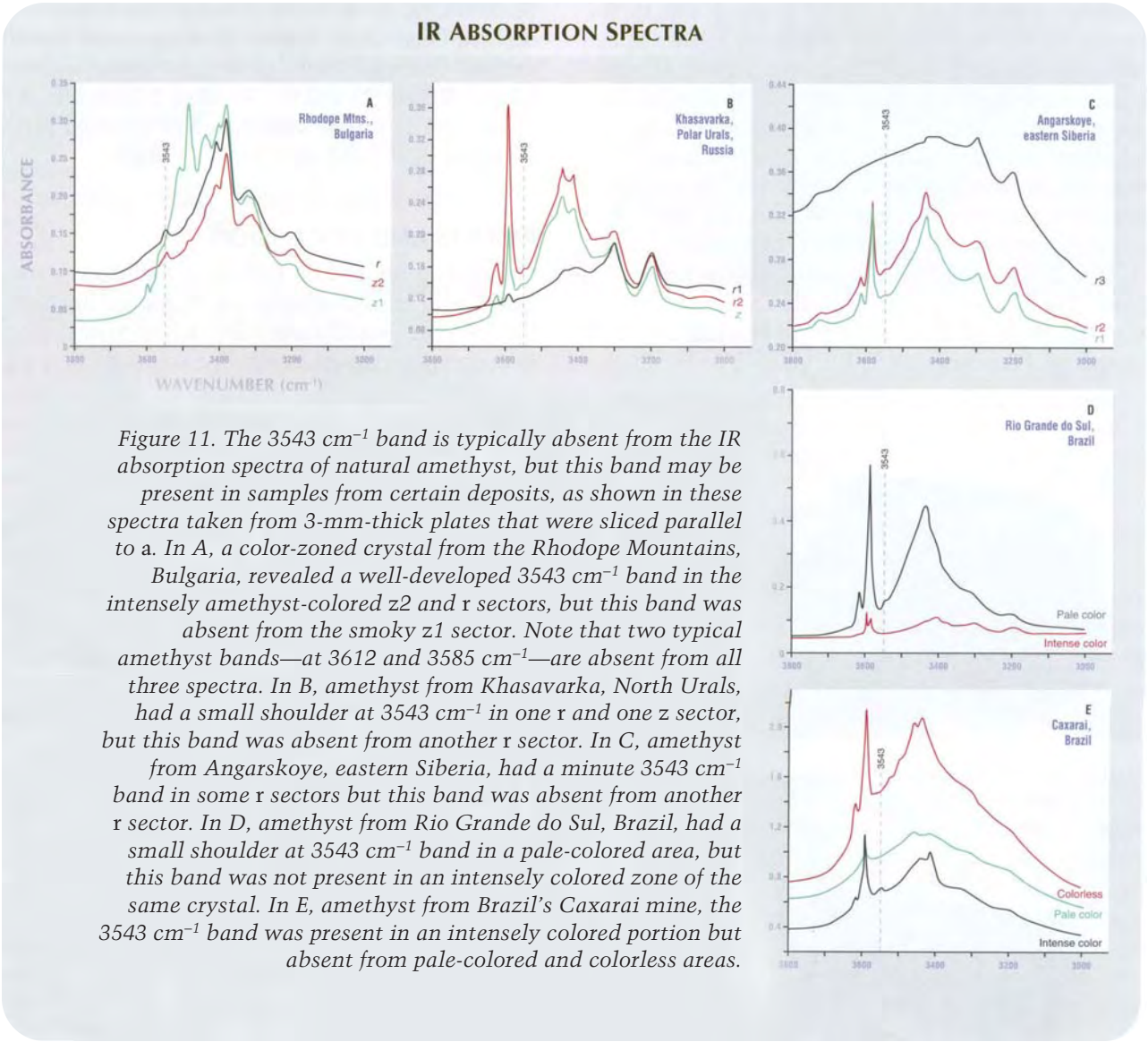

Figure 11. The 3543 cm^{-1} band is typically absent from the IR absorption spectra of natural amethyst, but this band may be present in samples from certain deposits, as shown in these spectra taken from 3-mm-thick plates that were sliced parallel to a. *In A, a color-zoned crystal from the Rhodope Mountains, Bulgaria, revealed a well-developed 3543 cm^{-1} band in the intensely amethyst-colored* z2 *and* r *sectors, but this band was absent from the smoky* z1 *sector. Note that two typical amethyst bands—at 3612 and 3585 cm^{-1}—are absent from all three spectra. In B, amethyst from Khasavarka, North Urals, had a small shoulder at 3543 cm^{-1} in one* r *and one* z *sector, but this band was absent from another* r *sector. In C, amethyst from Angarskoye, eastern Siberia, had a minute 3543 cm^{-1} band in some* r *sectors but this band was absent from another* r *sector. In D, amethyst from Rio Grande do Sul, Brazil, had a small shoulder at 3543 cm^{-1} band in a pale-colored area, but this band was not present in an intensely colored zone of the same crystal. In E, amethyst from Brazil's Caxarai mine, the 3543 cm^{-1} band was present in an intensely colored portion but absent from pale-colored and colorless areas.*

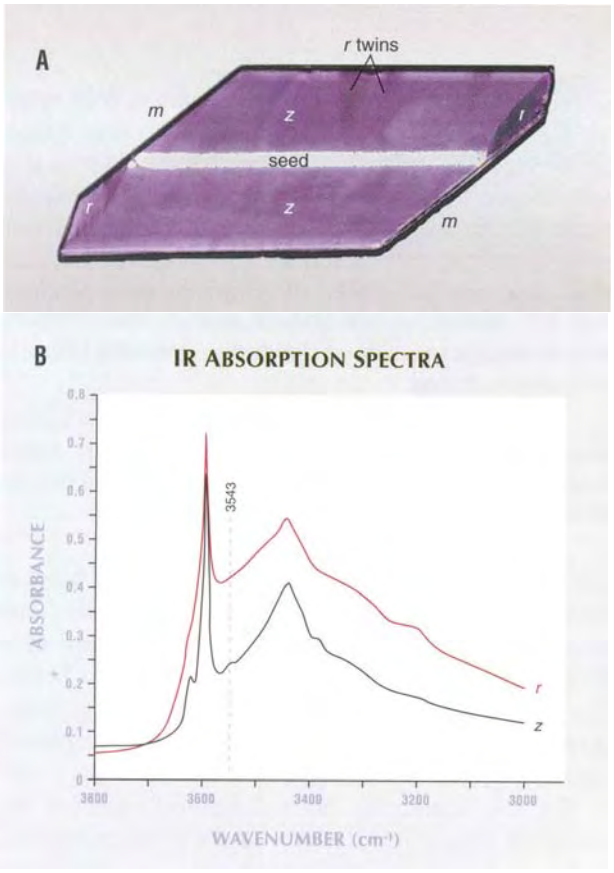

Figure 12. This synthetic amethyst plate in image A (3 mm thick and 7.3 cm long, sliced parallel to a*), grown in an alkaline solution on a seed plate cut parallel to* z*, provides an example of Condition 1. Before irradiation, the* z *sectors were colorless and the* r *sectors were pale yellow. Then, as shown in image A after irradiation, the* z *sectors became purplish violet and the* r *sectors turned very dark purple. The IR spectra in part B demonstrate that the 3543 cm^{-1} band was present in the* z *sectors, but absent from the* r *sectors. Photo by D. V. Balitsky.*

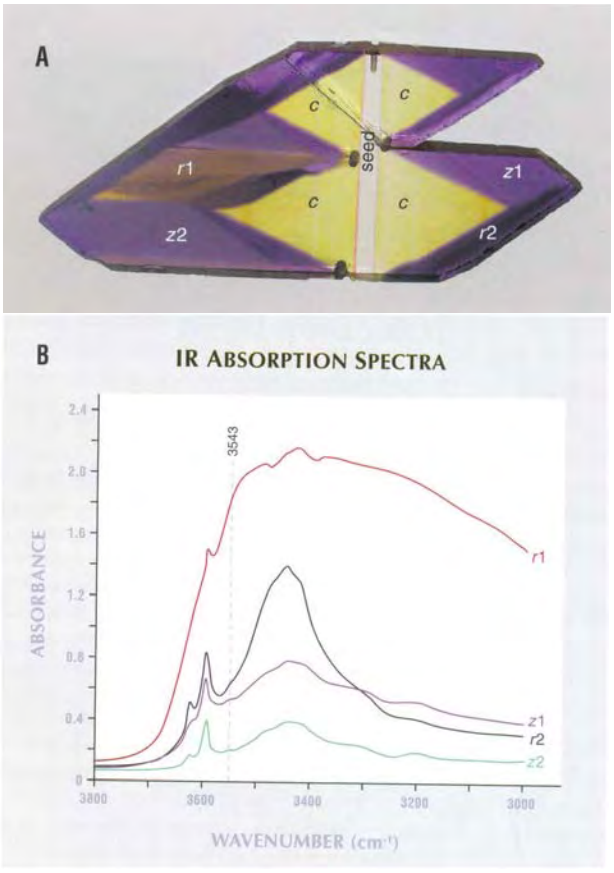

Figure 13. As another example of Condition 1, the plate of synthetic ametrine in image A (3 mm thick and 8 cm long, cut parallel to a*) was grown in an alkaline solution on a seed cut parallel to* c*. Before irradiation, the* z *sectors were very pale yellow, and the* r1 *sectors were yellow, with slightly more intense color in the* r *sector (i.e., it contained more citrine-forming impurities). As seen here after irradiation, the* z *sectors turned purple-violet, whereas the* r *sectors turned brownish yellow (sector* r1*) and very dark purple (sector* r2*). The IR spectra in part B show that the 3543 cm^{-1} band was absent from the* r *sectors, and barely present (to various degrees) in the* z *sectors. Photo by D. V. Balitsky.*

Relation to Growth Sectors in Synthetic Amethyst. In the colorless as-grown crystals that were produced in alkaline K_2CO_3 solutions, the 3543 cm^{-1} band was either completely absent or occurred only rarely as a very weak peak or a shoulder. However, our investigations revealed four conditions (according to the *z* and *r* growth sectors) that govern the presence and absence of the 3543 cm^{-1} band in synthetic amethyst grown in alkaline solutions after irradiation to produce the amethyst color. Although the four conditions described below indicate extreme situations, gradational characteristics also are possible according to variations in the growth conditions (a full list is available in the *G&G* Data Depository at www.gia.edu/gemsandgemology).

Condition 1. The 3543 cm^{-1} absorption band is present in the *z* sectors and absent from the *r* sectors (figures 12 and 13). This was the case for about 70–80% of the studied samples.

For this condition, the *z* sectors are colorless or very pale yellow before irradiation. This confirms that these sectors did not contain significant citrine-forming impurities (Balitsky and Balitskaya, 1986). In contrast, *r* sectors (as well as Dauphiné *r*-twins) within the same crystals initially are pale yellow to pale yellowish brown. With irradiation they become amethystine, sometimes with a barely visible

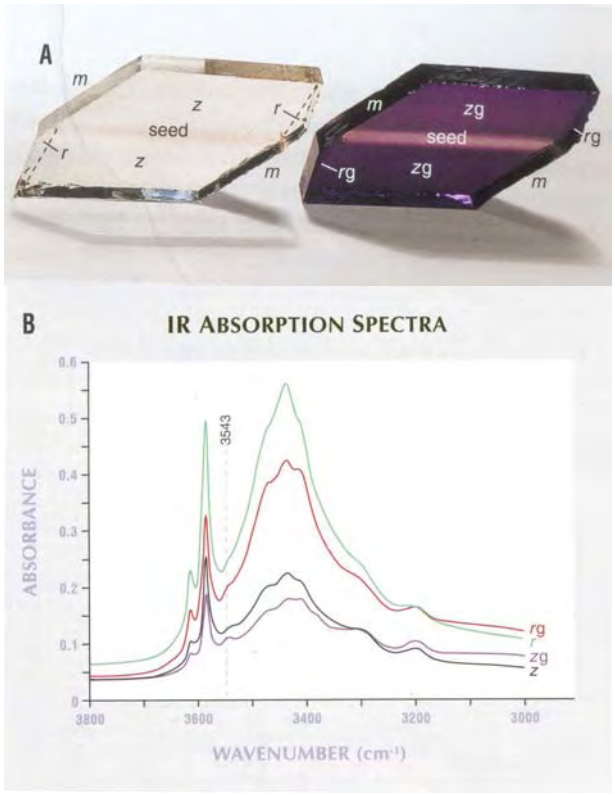

Figure 14. To illustrate Condition 2, image A shows plates of synthetic amethyst (3 mm thick and 7 cm long, sliced parallel to a*) that were grown in alkaline solutions on seeds cut parallel to* z*. Before irradiation, both the* z *and* r *sectors were colorless, indicating that they contained no citrine-forming impurity. After irradiation, both rhombohedral growth sectors became purple-violet (somewhat darker in the* r *sectors). The IR spectra in part B show that before irradiation, the 3543 cm^{-1} band was hardly noticeable (as a shoulder) in the* z *sectors, and was absent from the* r *sectors (labeled* z *and* r*, respectively). After gamma-irradiation, this band became distinct in the* z *sectors and appeared as a shoulder in the* r *sectors (*zg *and* rg*, respectively). Photo by V. S. Balitsky.*

brownish tint. This proves that the *r* sectors, as well as the Dauphiné *r*-twins, contain both citrine- and amethyst-forming impurities (Balitsky and Balitskaya, 1986).

In the example shown in figure 13, the citrine-forming impurity is only absent from the *z* sectors, and their IR spectra include the 3543 cm^{-1} band. However the *r* sectors captured more of the citrine-forming impurity and acquired a primary yellow to yellow-orange color. After gamma irradiation, they changed to brownish yellow (sector *r*1) and very dark reddish violet (sector *r*2).

According to our data, this situation was most common for synthetic amethyst grown during the 1970s and '80s in Russia. We have observed over the last decade that the amount of synthetic amethyst with a colorless *z* growth sector before irradiation was reduced by as much as 20–30%. We believe that this may be related to efforts to raise production by increasing the growth rate of the crystals, which results in more of the citrine-forming impurity being captured.

The samples of synthetic amethyst from China (grown in the 1980s) and Japan showed the same features; for all practical purposes, they could not be distinguished from the Russian material.

Condition 2. Less commonly, the 3543 cm^{-1} band is present in both the *z* and *r* sectors (figure 14). This was shown by about 20–30% of the Russian synthetic amethyst we studied that was grown before the 1990s and by nearly 40–50% of later production. We saw analogous IR spectra in our samples of Japanese synthetic amethyst.

For this condition, both the *z* and *r* sectors are colorless before irradiation—and therefore contain only structural amethyst-forming impurities. We have also noted intermediate cases in which the *z* sectors are perfectly colorless but the *r* sectors are very pale yellow before irradiation. This indicates the presence of traces of the nonstructural citrine-forming impurity. After irradiation, both rhombohedral growth sectors become purple-violet, but the *r* sectors have a somewhat darker color (and also a smaller 3543 cm^{-1} band).

Condition 3. Very rarely, the 3543 cm^{-1} band is absent from both the *z* and *r* sectors (figure 15). In this case, before irradiation both sectors are pale yellow to yellow or brownish yellow, which shows the presence of a citrine-forming impurity (in addition to an amethyst-forming impurity). After irradiation, both growth sectors become purple-violet, sometimes with a brownish tint. The intensity of this tint increases according to the amount of the citrine-forming impurity.

According to information from Dr. Liu Guobin (pers. comm., 1998) almost all Chinese synthetic amethyst grown on *z* seeds was pale yellow to yellow before irradiation. Our examination confirmed that the as-grown yellow color of Chinese synthetic amethyst also is caused by nonstructural iron impurities. In such material, the 3543 cm^{-1} band is absent from both the *z* and *r* sectors.

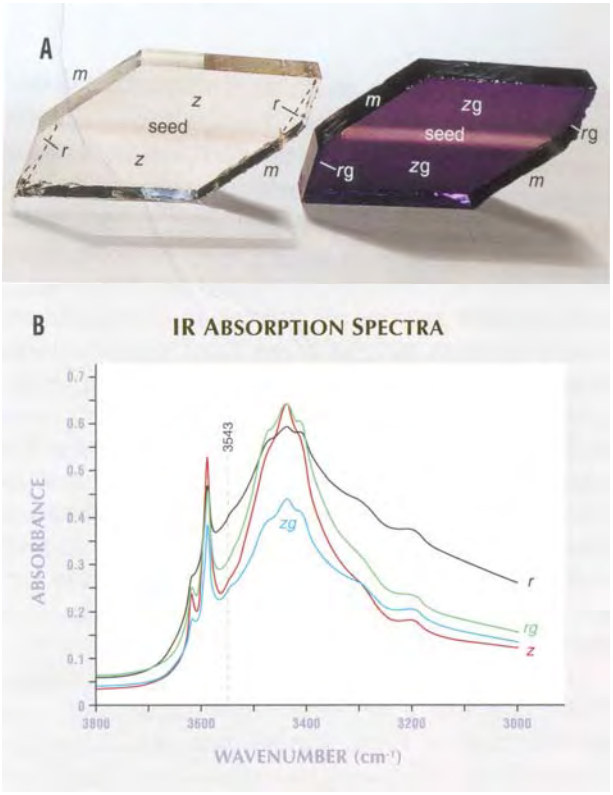

Figure 15. In part A, these plates of synthetic amethyst (10 mm thick and 6.0 cm long, sliced parallel to a*) were grown in alkaline solutions on seed plates cut parallel to* z*. They illustrate Condition 3. As grown, the rhombohedral sectors were pale yellow. With irradiation, the* r *and* z *sectors became purple-violet with a brownish tint, with the* r *sectors being somewhat darker in color. In part B, the 3543 cm^{-1} band is absent (or present as a hardly noticeable shoulder) in the IR spectra of the rhombohedral sectors, both before (*z *and* r*) and after irradiation (*zg *and* rg*). Photo by V. S. Balitsky.*

Condition 4. Also very rarely, the 3543 cm^{-1} band occurs in reverse of the first condition—that is, the band is present in the *r* sectors and absent from the *z* sectors. This situation arises when both amethyst- and citrine-forming impurities are present in the *z* sectors, but the *r* sectors have only the amethyst-forming impurity. In the authors' experience, such conditions are seldom encountered in the commercial growth of synthetic amethyst.

Thus, according to our data, the 3543 cm^{-1} band in the IR spectra of commercially available synthetic amethyst that has been grown in alkaline solutions almost always manifests itself in the *z* sectors and is often absent from the *r* sectors.

From these data and communications with other producers (e.g., in South Korea), we believe that more than 98% of the synthetic amethyst currently produced in Russia and other countries is grown on seeds cut parallel to *z*. This is because such crystals grow much faster than when seeds cut parallel to *r* are used. When grown on the *z*-seeds, the vast majority of such crystals are comprised of *z* sectors (see, e.g., figure 3B). *This is why the 3543 cm^{-1} band is found in the IR spectra of the majority of synthetic amethyst in the international gem trade.*

Effect of Growth Rate, Temperature, and Pressure. Our data show that the presence or absence of the 3543 cm^{-1} band in the IR spectra of synthetic amethyst grown in alkaline solutions mainly depends on the growth rates of the crystals. Growth rates are primarily a function of the pressure/temperature parameters, thermal gradient, composition of the solution, supersaturation, crystallographic orientation of the seed plates, and the position of the seed plates in the autoclave.

Because commercial growth processes maintain the solution at a constant composition, growth-rate variations mainly relate to the seed orientation (e.g., cut parallel to *z* or *r*) and the position of the seed in the autoclave relative to gravity. Depending on the pressure-temperature (P-T) conditions and temperature gradient, growth rates of the *z* face can exceed those of the *r* face by 5–8 times or more. However, the orientation of the seed relative to gravity and the temperature gradient can even affect the growth rates of faces with the *same* crystallographic orientation, especially the *r* faces, by a factor of 10 or more (see, e.g., the crystal in figure 13A). Moreover, slight deviations in the specified P-T conditions, especially the temperature gradient (i.e., solution supersaturation), also can affect the growth rates of both rhombohedra.

Balitsky and Balitskaya (1986) described the distribution of amethyst- and citrine-forming impurities in synthetic quartz according to the growth rates of the *z* and *r* faces. In particular, these faces capture the citrine-forming impurity in addition to the amethyst-forming impurity when they reach their "critical" growth rates. As mentioned above, the presence of the 3543 cm^{-1} band (in natural amethyst, as well as in synthetic amethyst grown in alkaline solutions) correlates to the presence of the amethyst-forming impurity, whereas its absence correlates to the simultaneous presence of both amethyst- and citrine-forming impurities.

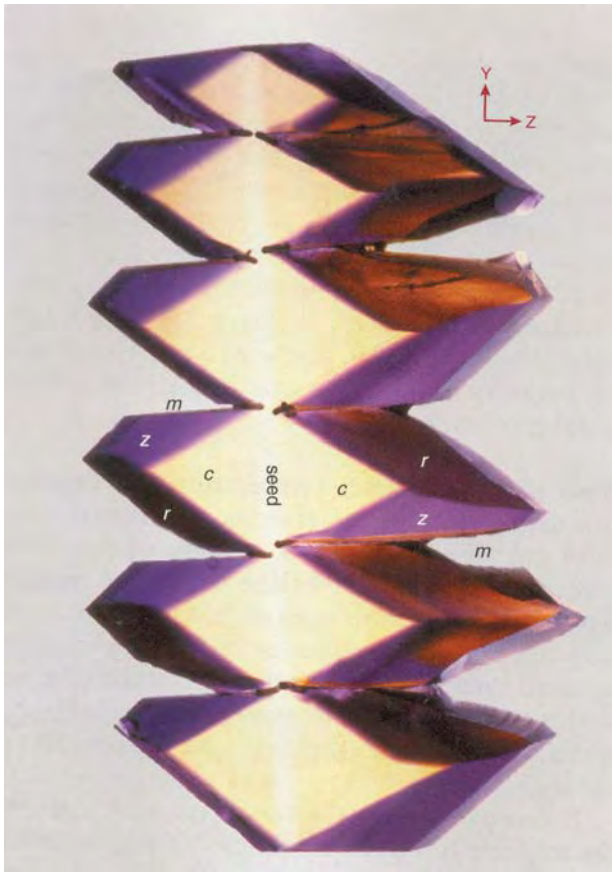

Figure 16. This plate of synthetic ametrine crystals (approximately 6.0 × 11.0 cm) was grown in an alkaline solution on a seed plate cut parallel to c. *The seed was oriented parallel to the vertical axis of the autoclave during crystal growth. In the different crystals, the growth rate of the* z *and, especially, the* r *faces was more rapid on the top than the bottom surfaces, to varying degrees. Faster growth rates caused greater incorporation of the citrine-forming impurities. Photo by V. S. Balitsky.*

This accounts for the fact that when the growth rate is below the critical rate (i.e., under conditions that capture the amethyst-forming impurity almost exclusively), the 3543 cm^{-1} band is present. However, as the critical rate is approached, the intensity of the 3543 cm^{-1} band first decreases and ultimately disappears if the growth rate is increased.

The commercial technology used to grow high-quality synthetic amethyst requires that the seeds be cut parallel to *z*. In this situation, the *z* faces usually do not attain the critical growth rate. We propose that this is the main reason why the 3543 cm^{-1} band is present in the overwhelming majority of synthetic amethyst, which predominantly consists of *z* sectors. However, with this seed orientation the *r* faces reach their own critical rate faster than the *z* faces, and will simultaneously capture both the amethyst- and citrine-forming impurities. This explains why in our samples this band was typically absent from the *r* sectors in the same crystals or in crystals grown on seed plates cut parallel to *r* in the same autoclave. Note that if both *z* and *r* sectors are present in a faceted synthetic amethyst, the 3543 cm^{-1} band will be detected only in certain portions of the sample.

We should emphasize, however, that various technological methods can be used to change the growth rates of the *z* and *r* faces, even within separate crystals in an autoclave (figure 16). Growth rates of these faces will decrease as pressure and, especially, temperature decrease. Thus, manufacturers can predetermine and control the presence or absence of the 3543 cm^{-1} band in synthetic quartz.

Our observations confirm previous findings on the relationship between these factors and the growth rates of these sectors in natural ametrine (Lemmlein, 1951) and in natural amethyst that develops a near-citrine color after thermal treatment (Nassau, 1981, 1994). This provides strong evidence that growth rate is important for determining the presence or absence of the 3543 cm^{-1} band in the IR spectra of natural, as well as synthetic, amethyst.

Effect of Crystallographic Orientation. To determine the effect of crystallographic orientation on the behavior of the 3543 cm^{-1} band, IR spectra were recorded from oriented cubes and plates cut perpendicular to those described in the preceding section, for both natural and synthetic amethyst. We found that the occurrence of the 3543 cm^{-1} band did not depend on crystallographic orientation (figure 17). However, due to polarization, we observed a change in the intensity of this band.

Effect of Irradiation and Annealing. As noted earlier, the 3543 cm^{-1} band was either completely absent or occurred rarely as a hardly noticeable peak or a shoulder in the colorless as-grown (i.e., non-irradiated) crystals produced in alkaline K_2CO_3 solutions. However, after irradiation to produce the amethyst color, this band appeared distinctly in the IR spectra of the majority of synthetic amethysts (see figures 14 and 18). This band could be eliminated by heat treatment (i.e., at 420°C) to remove the amethyst color, and then be restored by subsequent irradiation to bring back the amethyst color (again, see figure 18).

As a rule, synthetic amethyst grown in alkaline

solutions contains Al-alkaline centers in addition to the predominant amethyst color centers (Rossman, 1994). These Al-alkaline centers manifest themselves through irradiation by giving a smoky tint (figure 19). According to our data, the smoky color centers in such crystals can be destroyed by annealing at 300–310°C for one hour. Although the smoky tint disappears, the amethyst color and the 3543 cm^{-1} band remain. However, after further heat treatment at 450°C for two hours, both the amethyst color and the 3543 cm^{-1} band disappear completely. Subsequent gamma irradiation restores the amethyst–smoky quartz color, and the 3543 cm^{-1} band re-appears in the IR spectra.

Nevertheless, there appears to be no direct relationship between amethyst color and the 3543 cm^{-1} band. Our experiments show that the 3543 cm^{-1} band also occurs in the IR spectra of gamma-irradiated synthetic smoky quartz that was grown in iron-free sodium alkaline solutions on seed plates cut parallel to *z* (Balitsky et al., 2003). In this case, the 3543 cm^{-1} band is present only in synthetic quartz crystals that attain a growth rate on the order of 0.4–0.5 mm/day—that is, close to that of commercially produced synthetic amethyst. By analogy to synthetic amethyst, the 3543 cm^{-1} band in such

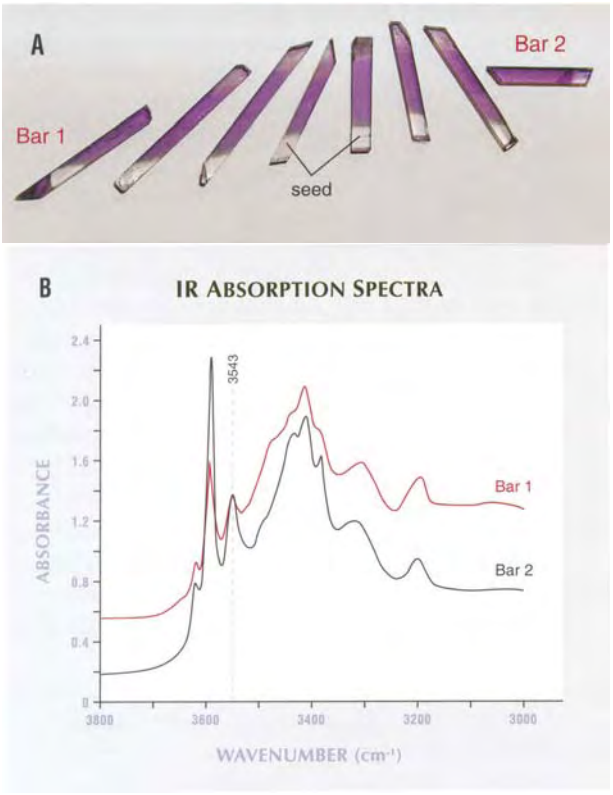

Figure 17. The bars in image A (each 2 mm thick; bar 2 is 2.0 cm long) were cut in various orientations (differing by approximately 10°) from the same plate of synthetic amethyst, which was sliced parallel to a. *The crystal was grown in an alkaline solution on a seed plate cut parallel to* z. *As shown in part B, the 3543 cm^{-1} band was clearly visible in the IR spectrum of these representative samples, regardless of their orientation. The change in the intensity of this band was due to polarization effects. Photo by D. V. Balitsky.*

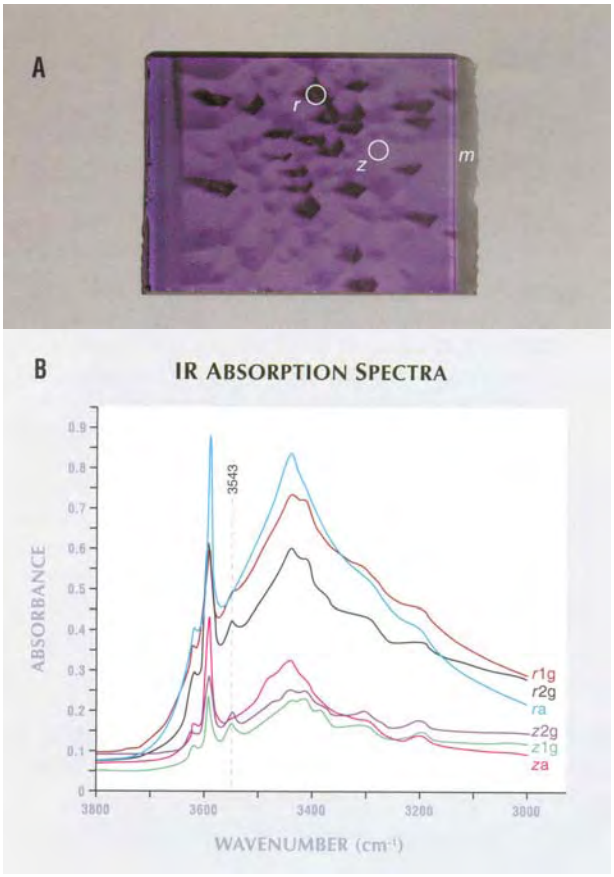

Figure 18. The sample of synthetic amethyst in image A (2.5 mm thick, 5.0 cm wide, sliced parallel to z*) was grown in an alkaline solution on a seed plate cut parallel to* z. *Numerous Brazil* r*-twins (dark areas) are present in this* z *sector. Before irradiation, the plate was colorless and the 3543 cm^{-1} band was absent from both the* z *and* r *sectors. However, as shown in part B, this band appeared in the spectra of these sectors after gamma irradiation (*z*1g and* r*1g). After annealing at 420°C for two hours, this band practically disappeared (*z*a and* r*a), but after irradiation it appeared again (*z*2g and* r*2g). The spectra were recorded from the same locations on the sample, as labeled. Photo by D. V. Balitsky.*

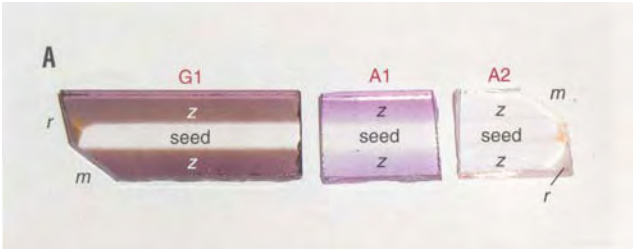

Figure 19. This slice of synthetic quartz (3 mm thick, up to 6.5 cm long, sliced parallel to a*) was cut into three pieces for irradiation and heat-treatment experiments (see image A). The original crystal was grown in an alkaline solution on a seed plate cut parallel to* z*. As grown, the* z *sectors were colorless, but with irradiation they turned smoky violet (sample G1). Annealing at 310°C for one hour left a pale amethyst color (sample A1). The 3543 cm^{-1} band, though weak, was present in the spectra of both samples (see part B). However, after annealing at 450°C for two hours, the synthetic quartz became completely colorless (sample A2) and the band at 3543 cm^{-1} disappeared. Photo by D. V. Balitsky.*

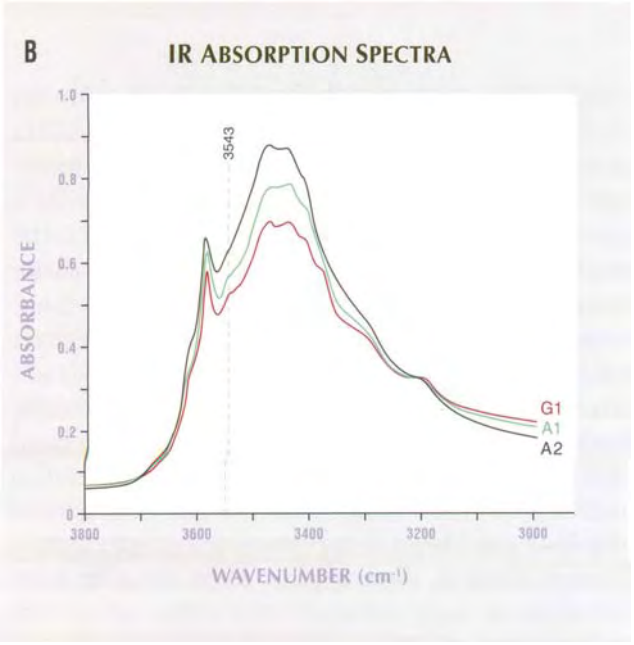

material disappears when it is annealed at 450°C for two hours. This band also is absent from synthetic quartz produced under the same conditions, but with a slower growth rate (0.2 mm/day), although

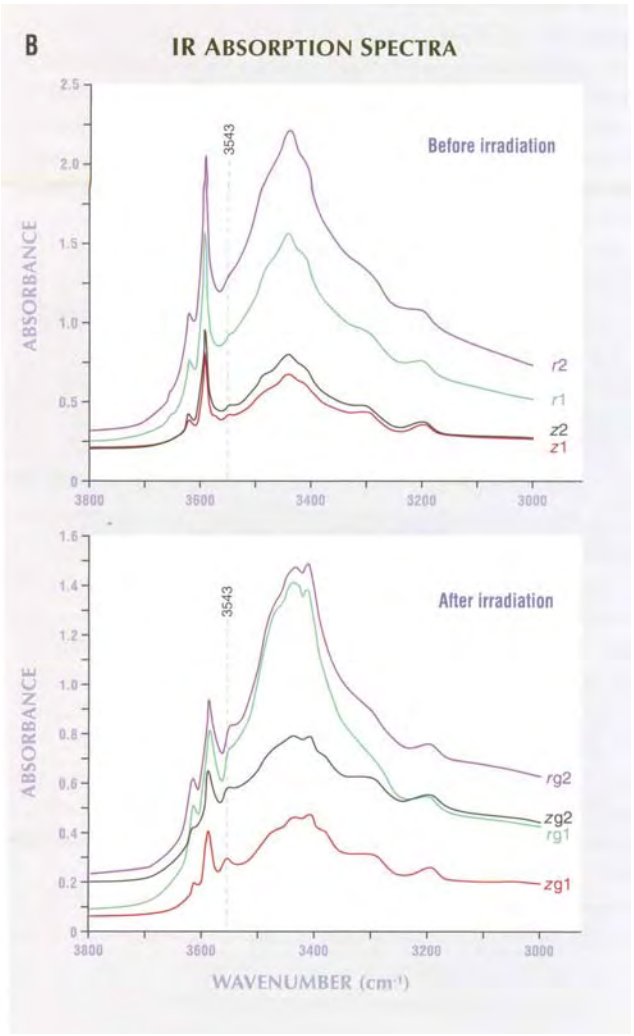

Figure 20. The plates of multicolored synthetic quartz in image A (2.5 mm thick and 6.0 cm tall, sliced parallel to a*) were cut from the same crystal, which was grown in an alkaline solution on a seed plate cut parallel to* c*. The multicolored nature is related to a decrease of oxygen potential in the solution (Balitsky et al., 1999). Before irradiation (left plate), both the* z *and* r *sectors were colorless or pale yellow, and the 3543 cm^{-1} band was present as a very weak peak or shoulder, as seen in part B. After irradiation (right plate), the inner zones of the* z *and* r *sectors became purplish violet but their outer zones remained almost colorless. Nevertheless, the 3543 cm^{-1} band was seen in the IR spectra of both the purplish violet and near-colorless zones. Photo by D. V. Balitsky.*

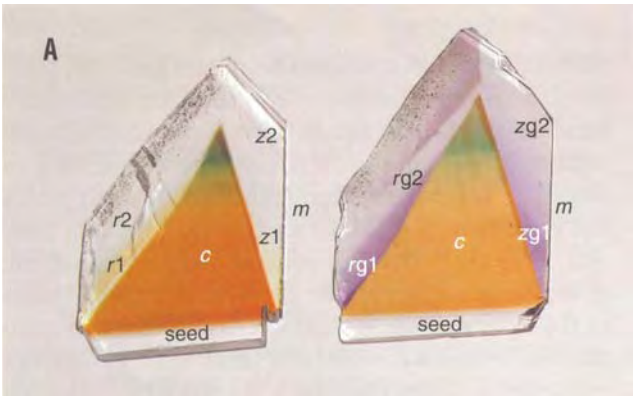

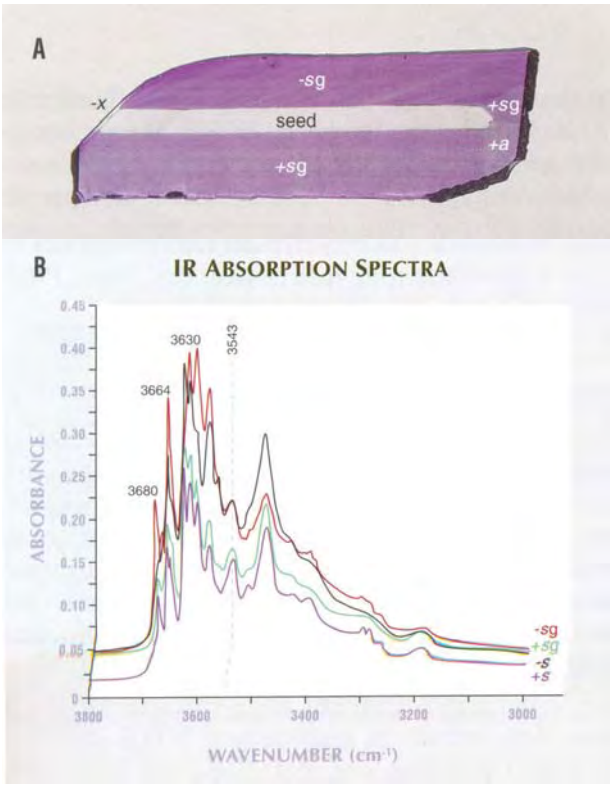

Figure 21. The synthetic amethyst in image A (2.0 mm thick and 2.3 cm long, sliced in ZX-orientation) was grown in an NH_4F solution on a seed plate cut parallel to s*. In part B, typical IR absorption spectra are shown for both the* +s *and* –s *sectors. Several of the peaks (especially at approximately 3680, 3664, and 3630 cm^{-1}) are not found in the spectra of natural or alkaline-solution-grown synthetic amethyst. Note that the 3543 cm^{-1} band was present both before (*+s, –s*) and after irradiation (*+sg, –sg*). Photo by D. V. Balitsky.*

two other characteristic bands at 3612 and 3585 cm^{-1} are present in that case.

Additional evidence for the lack of any correlation between amethyst color and the 3543 cm^{-1} band is found in plates of the multicolored brownish yellow–green–amethyst synthetic quartz before and after irradiation (figure 20).

Thus, our studies show that the 3543 cm^{-1} band in the IR spectra of natural amethyst and of synthetic amethyst grown in alkaline solutions is probably associated with specific OH^- defects that manifest themselves in the quartz structure under the effect of ionizing irradiation.

Effect of Solution Composition. The IR spectra of synthetic amethyst grown in near-neutral NH_4F solutions show unique absorption features (figures 21 and 22). In particular, such crystals show clear

Figure 22. The plate of synthetic amethyst in image A (2 mm thick and 3.0 cm long, sliced parallel to m*) was grown in an NH_4F solution on a seed plate cut parallel to* c*. After irradiation, it was cut into three pieces (image B) that were subjected to heat treatment at 500°C (sample c1), 600°C (sample c2) and 700°C (sample c3). In the IR spectra shown in part C, the unheated sample showed a broad band with a maximum near 3400 cm^{-1} (related to molecular water). This band was not present in the heated samples, although numerous other bands in the 3700–3550 cm^{-1} region—including the 3543 cm^{-1} band—did not undergo any changes. Photo by D. V. Balitsky.*

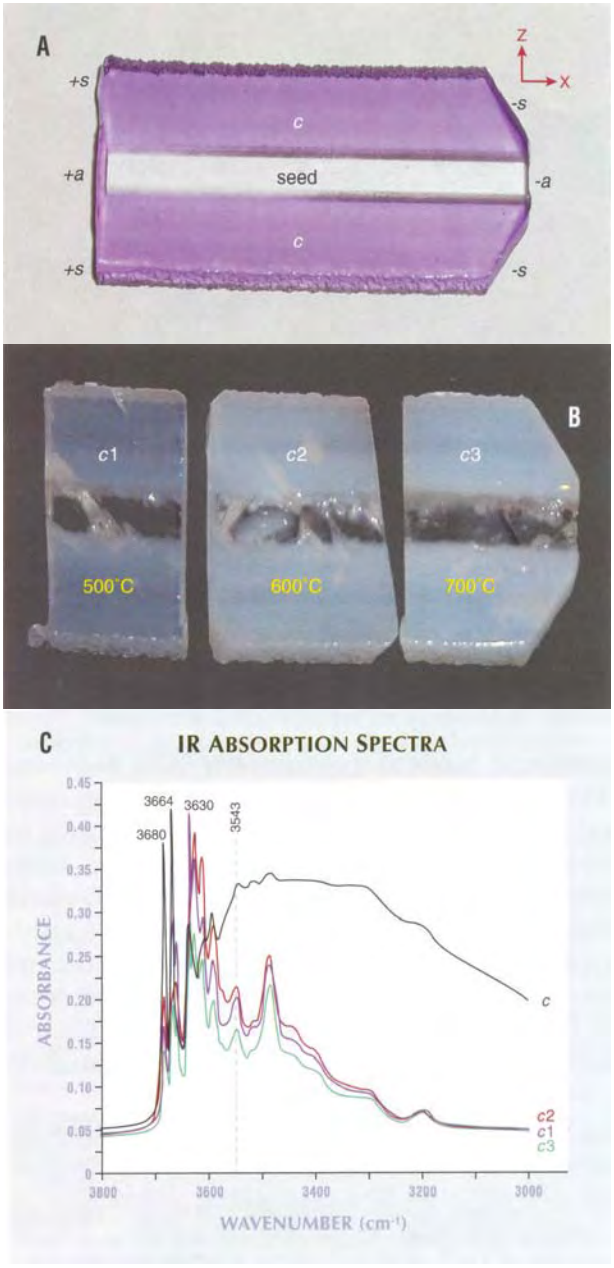

Figure 23. Synthetic amethyst has been produced in large quantities for the gem trade, but it remains challenging to identify. The synthetic amethyst shown here is set in a pendant with pavé diamonds. The unmounted oval brilliant weighs 5.56 ct (GIA Collection no. 13438B). Jewelry courtesy of Gems of La Costa, Carlsbad, California; photo by Maha Tannous.

absorption bands at approximately 3680, 3664, and 3630 cm^{-1} that never manifest themselves in natural amethyst or in synthetic amethyst grown in alkaline solutions (Balitsky, 1980; Balitsky, 1981; Balitsky et al., 2000). Also present are more subtle bands at 3606, 3590, 3543, 3513, and 3483 cm^{-1}. Our experiments indicate that the position and intensity of all eight bands, including the one near 3543 cm^{-1}, are not affected by the irradiation and annealing described above for synthetic amethyst grown in alkaline solutions.

Synthetic amethyst that is grown in NH_4F solutions at low temperature (240–300°C) and low pressure (80 atm) conditions contains a high concentration of molecular water (Balitsky, 1981). The IR spectra of such material show a broad band with a maximum near 3400 cm^{-1} (again, see figure 22). After thermal treatment at 450°C for four hours, the amethyst color disappears, and at higher temperatures (500–700°C) the synthetic quartz becomes milky. This phenomenon, which is related to molecular water, is typical for all varieties of high-water-containing quartz (see, e.g., Kats, 1962; Balakirev et al., 1979; Rossman, 1988).

CONCLUSIONS

Despite its prevalence in the gem and jewelry trade (figure 23), synthetic amethyst remains difficult to separate from its natural counterpart. Infrared spectroscopy has limited usefulness in this distinction. The presence of an absorption band near 3595 cm^{-1} is indicative of natural amethyst (Zecchini, 1999), but not all natural amethyst shows this band. An absorption band at 3543 cm^{-1} can confirm the synthetic origin of amethyst grown in near-neutral NH_4F solutions (together with bands at 3680, 3664, and 3630 cm^{-1}), but it cannot be used to positively distinguish the material grown in alkaline solutions.

Currently, most commercial synthetic amethyst is grown in alkaline solutions, on seeds cut parallel to *z*, at growth rates that usually exclude the capture of the citrine-forming impurity. It is primarily for this reason that the 3543 cm^{-1} band is present in the IR spectra of the overwhelming majority of synthetic amethyst. However, very often this band is absent from the *r* sectors in the same crystals, or from crystals that are grown on seeds cut parallel to *r*. Due to initiatives to increase production by using faster growth rates on seeds cut parallel to *z*, such crystals would be expected to simultaneously capture both amethyst- and citrine-forming impurities. Accordingly, the 3543 cm^{-1} band would not be detected in the IR spectra of material faceted from such crystals.

In addition, the 3543 cm^{-1} band is not as rare in natural amethyst as commonly believed. Its presence in such material is probably also caused by slower growth rates of the rhombohedral faces, resulting in only minor capture of the nonstructural citrine-forming impurities. Nevertheless, natural amethyst is mainly formed by *r* growth sectors that typically capture more nonstructural citrine-forming impurities than the *z* growth sectors. Therefore, the 3543 cm^{-1} band is much less common in natural amethyst than in synthetic material.

On the whole, while the presence of an absorp-

tion band at approximately 3543 cm^{-1} may be considered indicative of possible synthetic origin, it cannot be used for the positive identification of synthetic amethyst. Therefore, the unambiguous identification of natural versus synthetic amethyst must be based on a combined examination of the IR spectra, internal growth structures (e.g., characteristics of Dauphiné and Brazil twins, presence of particular growth sectors and zones, as well as a stream-like structure seen in synthetic amethyst), and inclusions (e.g., presence of chlorides, barite, calcite, and multiphase fluid inclusions in natural amethyst).

ABOUT THE AUTHORS

Dr. V. S. Balitsky (balvlad@iem.ac.ru) is head of the Laboratory for Mineral Synthesis and Modification of Minerals, and Dr. Bondarenko is head of the Laboratory for Physical-Chemical Investigation, at the Institute of Experimental Mineralogy, Russian Academy of Science, Chernogolovka, Moscow District, Russia. Dr. D. V. Balitsky is a researcher in the Physical-Chemical Laboratory of Condensate Materials at Université Montpellier II, France. Dr. O. V. Balitskaya is senior researcher at the Fersman Mineralogical Museum, Moscow.

ACKNOWLEDGMENTS: The authors are grateful to Dr. Yu. P. Belyakova, Dr. A. A. Mar'in, and Dr. I. B. Makhina (VNIISIMS, Aleksandrov), and Dr. Liu Guobin (retired, Wushan, China), for help in obtaining some samples of synthetic amethyst, as well as to Dr. V. V. Boukanov (St. Petersburg), Dr. T. Lu (GIA, Carlsbad), Dr. H. Kitamaki (All-Japan Gemmological Association, Tokyo), and Dr. M. M. Maleev (Museum of Crystals, Sofia, Bulgaria) for providing samples of natural amethyst from various deposits. This work is supported by two grants (Nos. 03-02-16613 and 03-03-32950) from the Russian Basic Research Foundation.

REFERENCES

Balakirev V.G., E.Ya. Kievlenko, L.V. Nikolskaya, Samoilovich M.I., Khadji V.E., Tsinober L.I. (1979) *Mineralogy and Crystal Physics of the Gem Varieties of Silica*. Nedra Publishers, Moscow (in Russian).

Balitsky V.S. (1980) Synthetic amethyst: Its history, methods of growing, morphology, and peculiar features. *Zeitschrift der Deutschen Gemmologischen Gesellschaft*, Vol. 29, No. 1/2, pp. 5–16.

Balitsky V.S. (1981) Gemmology of some colored varieties of synthetic quartz. *Journal of the Gemmological Society of Japan*, Vol. 8, No. 1–4, pp. 103–117.

Balitsky V.S., Lisitsina E.E. (1981) *Synthetic Analogues and Imitations of Natural Gems*. Nedra Publishers, Moscow (in Russian).

Balitsky V.S., Balitskaya O.V. (1985) Two-colored amethyst-citrine quartz and conditions of its formation. *Proceedings of the Russian Mineralogical Society*, Vol. 64, No. 6, pp. 664–676 (in Russian).

Balitsky V.S., Balitskaya O.V. (1986) The amethyst-citrine dichromatism in quartz and its origin. *Physics and Chemistry of Minerals*, Vol. 13, pp. 415–421.

Balitsky V.S., Lu T., Rossman G.R., Makhina I.B., Mar'in A.A., Shigley J.E., Elen S., Dorogovin B.A. (1999) Russian synthetic ametrine. *Gems & Gemology*, Vol. 35, No. 2, pp. 122–134.

Balitsky B.S., Makhina I.B., Marina E.A., Kolodieva S.V. (2000) Synthesis of quartz and some of its colored varieties in the fluoride solutions. In *Mineral Synthesis*, 2nd ed., Vol. 1, VNIISIMS, Aleksandrov, pp. 175–229 (in Russian).

Balitsky V.S., Balitskaya O.V, Bondarenko G.V., Balitsky D.V. (2003) IR-spectroscopic characteristics of natural and synthetic amethysts in the region of 3000–3700 cm^{-1} and their identification. *Gemological Bulletin*, No. 10, pp. 21–33 (in Russian).

Balitsky V.S., Bondarenko G.V., Balitskaya O.V, Balitsky D.V. (2004) IR spectroscopy of natural and synthetic amethysts in the 3000–3700 cm^{-1} region and problem of their identification. *Doklady Earth Sciences*, Vol. 394, No. 1, pp. 120–123.

Dana J.D., Dana E.S., Frondel C. (1962) *The System of Mineralogy*, 7th ed., Vol. III, Silica Minerals. John Wiley & Sons, New York, 334 pp.

Fritsch E., Koivula J.I. (1987) How to tell if that amethyst is natural. *Jeweler's Circular Keystone*, Vol. 153, No. 7, pp. 322–324.

Fritsch E., Rossman G.R. (1990) New technologies of the 1980s: Their impact in gemology. *Gems & Gemology*, Vol. 26, No. 1, pp. 64–75.

Kats A. (1962) Hydrogen in α-quartz. *Philips Research Reports*, Vol. 17, pp. 133–195.

Kitawaki H. (2002) Natural amethyst from the Caxarai mine, Brazil, with a spectrum containing an absorption peak at 3543 cm^{-1}. *Journal of Gemmology*, Vol. 28, No. 2, pp. 101–108.

Lemmlein G.G. (1951) Color distribution in quartz crystals. *Trudy Instituta Kristallografii Akademii Nauk SSSR*, Vol. 6, pp. 255–268 (in Russian).

Lind T., Schmetzer K. (1983) A method for measuring the infrared spectra of faceted gems such as natural and synthetic amethyst. *Journal of Gemmology*, Vol. 18, No. 5, pp. 411–420.

Nassau K. (1981) Artificially induced color in amethyst-citrine quartz. *Gems & Gemology*, Vol. 17, No. 1, pp. 37–39.

Nassau K. (1994) *Gemstone Enhancement*, 2nd ed. Butterworth-Heinemann, Oxford.

Rossman G.R. (1988) Vibrational spectroscopy of hydrous components. In F.C. Hawthorne, Ed., *Spectroscopic Methods in Mineralogy and Geology, Reviews in Mineralogy*, Mineralogical Society of America, Washington, D.C., Vol. 18, pp. 193–206.

Rossman G.R. (1994) Colored varieties of the silica minerals. In P.J. Heaney, C.T. Prewitt, and G.V. Gibbs, Eds., *Silica: Physical Behavior, Geochemistry and Materials Applications, Reviews in Mineralogy*, Mineralogical Society of America, Washington, D.C., Vol. 29, pp. 433–462.

Zecchini P. (1979) Étude de l'absorption infrarouge de quartz d'origine naturelle ou de synthèse. *Revue de Gemmologie a.f.g.*, No. 60, pp. 14–18.

Zecchini P., Smaali M. (1999) Identification de l'origine naturelle ou artificielle des quartz. *Revue de Gemmologie a.f.g.*, No. 138/139, pp. 74–83.